



Wear behaviors of electroplated CBN grinding wheel with orderly-micro-grooves in grinding narrow-deep slot

Cong Mao¹ · Xiang Li¹ · Mingjun Zhang¹ · Jian Zhang¹ · Weiyu Zhang² · Yuanqiang Luo¹ · Weidong Tang¹ · Kun Tang¹ · Zhuming Bi³ · Yongle Hu¹ · Zhenheng Lin⁴

Received: 9 August 2023 / Accepted: 11 October 2023 / Published online: 1 November 2023
© The Author(s), under exclusive licence to Springer-Verlag London Ltd., part of Springer Nature 2023

Abstract

A grinding wheel with orderly-micro-grooves is a new type of structured grinding wheel for grinding narrow-deep slots. It can improve the carrying capacity of the coolant in the grinding zone effectively. The wear and evolution of grains directly determine the sharpness of the grinding wheel, and this affects the grinding performance in terms of efficiency, surface integrity, and tool life. In order to design the grinding wheel for minimized wear in its use, this study elucidates the wear behaviors of the grinding wheel with orderly-micro-grooves in grinding narrow-deep slots. Through the comparative experiments of the grinding narrow-deep slot, the impacts of micro-grooves on the wear behaviors of the grinding wheel are evaluated, and the wear behavior of the grains on the cut-in edge, cut-out edge, cylindrical surface, and side surface is observed, respectively. The analysis of the grinding ratio, grinding force, and force ratio further verifies the analysis of the wear mechanism and the grinding performance. It is found that (1) the macro-fracture of grain on the cut-in edge occurred due to the large cutting thickness increasing the load of the grain; (2) the debonding phenomenon reduces the anchoring force of the grain, and this tends to pull out the grain on the cut-out edge; (3) due to the adhesion action of the micro-welds, the main failure behavior of the grain on the cylindrical surface is chip adhesion, and the bridge adhesion appears at the small inter-grain space; (4) grains on the side surface are less engaged in removing workpiece materials, the cutting depths of the grains in the middle and inner zones are ignorable, and attrition wears and micro-fractures occur on the grains on the side surface. The grinding force and force ratio variation further verifies that the grinding wheel with orderly-micro-grooves can achieve self-sharpening to maintain excellent grinding performance.

Keywords Electroplated grinding wheel · Orderly-micro-grooves · Wear behavior · Narrow-deep slot · Grain fracture

1 Introduction

With the growing need for precise machines in aerospace, defense, automobile, and construction machinery, parts with machined narrow-deep slots are widely used, and typically, a narrow-deep slot refers to a slot with a width of less than 2 mm and a high aspect ratio greater than 2 [1]. To achieve the desired high accuracy, super-abrasive grinding wheels are increasingly used to produce narrow-deep slots due to their superior grinding performance in terms of hardness, thermal conductivity, and wear resistance [2]. However, the narrow-deep slot causes the problem of using a coolant to remove debris and dissipate heat in the grinding zone effectively, and this further induces some surface defects such as burns, micro-fractures, adverse residual stresses, and deterioration of the grinding wheel.

✉ Mingjun Zhang
mj_zhang@csust.edu.cn

¹ Hunan Provincial Key Laboratory of Intelligent Manufacturing Technology for High-Performance Mechanical Equipment, Changsha University of Science and Technology, Changsha 410114, China

² China Railway Wuxin Heavy Industry Co., Ltd., Changsha 410199, China

³ Department of Civil and Mechanical Engineering, Purdue University Fort Wayne, Fort Wayne, IN 46805, USA

⁴ School of Mechanical and Electrical Engineering, Putian University, Putian 351100, China

To improve the carrying and conveying capability of the coolant in the grinding zone, significant efforts were carried out to study the texturing/patterning of conventional grinding wheels [3]. For example, Guo et al. [4] proposed a micro-structured coarse-grained wheel that was made by using laser technology, and the grinding experiments on optical glass showed a significant reduction in subsurface damages. Denkena et al. [5] presented a patterned grinding wheel, and the results showed that the grinding force was lowered by 20%. The intermittent grinding wheel with internal cooling by Shi et al. [6] reduced the grinding temperature by 57% in experiments. Tawakoli et al. [7] applied dressing operation to create designed structures on the grinding wheel surface and observed that the area-specific grinding energy was significantly reduced. Aurich et al. [8] also fabricated a grinding wheel with an internal coolant supply, which significantly improved the cooling efficiency as the coolant was supplied into the contact zone directly. Walter et al. [9] used a picosecond laser to produce various micropatterns on the surface of the cubic boron nitride (CBN) grinding wheel, and the results showed a reduction of grinding forces in a range between 25 and 54%. Mohamed et al. [10] used a single-point diamond dressing tool to cut shallow circumferential grooves on the surface of a grinding wheel, and the experiments showed that the grinding wheel increased the average undeformed chip thickness effectively. Oliveira et al. [11] produced patterns on the wheel surface during the dressing operation, and the grinding power was reduced significantly. Ding et al. [12, 13] developed open-porous sintered CBN abrasive wheels; this provided additional storage space for chips and improved the storage capacity for coolants simultaneously. Cao et al. [14] indicated that the intermittent cutting behavior caused a decrease in the contact length by 42%, resulting in a significant reduction of grinding temperature and grinding force by 40% and 41%. Yuan et al. [15] fabricated an electroplated CBN wheel with controlled abrasive clusters, and the phenomenon of wheel loading was reduced significantly. An electroplated grinding wheel with orderly-micro-grooves was designed in our previous studies [16], and the experiments showed a 25% reduction of the grinding temperature. However, there is a need to investigate the wear behaviors of the grinding wheel to further improve grinding efficiency and obtain good surface integrity.

Early studies on wear behaviors of super-abrasive grinding wheels focused on their impacts on the grinding performance. For example, Upadhyaya and Fiecoat [17] studied the effect of CBN crystal characteristics on the performance of an electroplated CBN wheel and found that overall wheel wear depended more on crystal exposure. Gift and Misiólek [18] considered the relationship between coolants and the wear occurring to a grinding wheel, and they concluded that the grinding force was the primary factor to fail the

water-based fluid. The radial wear of a grinding wheel is often used as an important factor to evaluate the degree of wheel wear. Cao et al. [19, 20] found that the employment of tangential ultrasonic vibration reduces the grinding ratio by 22% in creep-feed grinding, and the normal and tangential grinding forces decreased by 35% and 39% in comparison with conventional grinding. Hartig et al. [21] discussed the impact of the cutting depth on the wear of the grinding wheel and concluded that the radial wear exhibited an overall lower value at a small cutting depth. Zhang et al. [22] studied the residual stress on the workpiece surface with different grinding wheel speeds and feed speeds and found that the change in grinding wheel speeds had little influence on the residual stress. Azizi et al. [23] found that the radial wheel wear was due to bond fracture and grain pull-out. Naik et al. [24] characterized the progress of the growth of radial wear that began with an initial high wear rate, then was followed by a steady rise, and finally terminated by a rapid increase.

Due to the randomness of distribution and geometric shapes of abrasives over the surface of the wheel, workpiece materials are removed by accumulated actions of numerous abrasives, and this brings the challenge of quantifying the wear of a grinding wheel. Shi and Malkin [25] showed that the grain wear form of the electroplated grinding wheel included attrition, pull-out, and fracture of grains. Miao et al. [26, 27] found that the wear behaviors varied in different regions of a wheel in the creep-feed profile grinding of a turbine blade root. Naskar et al. [28] discovered that thermal shock was a dominant factor to cause the macro-fracture of CBN grains. Li et al. [29] found that attrition wear and micro-fracture are the main wear behaviors at the steady wear stage. Liu et al. [30] revealed the determination mechanism of any effective grain and workpiece under different microscopic contact states. Wang et al. [2] found that the micro-fractures near the cutting edges were caused by a combination of tensile and compressive stresses. Based on the analysis of topography and wear characteristics of a diamond wheel in a sharpening process, Li et al. [31] found that two predominant wear modes were (1) micro-fracture of diamond grains and (2) ductile removal of resin bond. Zhu et al. [32] analyzed the wear behavior of polycrystalline CBN grains and indicated that the micro-fractures of the PCBN grains were caused by the intergranular fractures of the grains. However, aforementioned studies were mainly on the wear behaviors of conventional grinding wheels; few studies were conducted on those of structured grinding wheels. The mechanism analysis of wheel wear on the structural grinding wheel still needs to be carried out sufficiently.

This paper aims to investigate the wear behaviors of the electroplated CBN grinding wheel with orderly-micro-grooves when it is used to grind narrow-deep slots by experiments. To evaluate the growth of wear, a 3D ultra-large

depth of field microscope is used to examine the morphology evolution of the grinding wheel. The wear of grains on a cut-in edge, cut-out edge, cylindrical surface, and side surface is measured to reveal the wear mechanisms of the grains in different regions. The impacts of the micro-grooves on the wear of the grinding wheel are investigated to optimize the performance of the designed grinding wheel.

2 Experimental procedure

Grinding experiments were conducted in an up-grinding mode on a surface grinding machine (MGK 7120 × 6, Hangzhou Machine Tool Co., Ltd., China). Water-based emulsion was used as a coolant. The grinding wheel has a diameter of 200 mm and a width of 4 mm. A total of 600 straight micro-grooves are distributed around the outer circumference surface of the wheel. The micro-grooves are 1.5 mm in depth, 0.1 mm in width, and 1.05 mm in interval, as shown in Fig. 1a. The CBN abrasives were bonded to the metallic substrate by nickel. The average diameter of abrasives is 96 μm. The grinding wheel was prepared with orderly-micro-grooves by following the instructions in [15]. Figure 1b shows the experimental setup.

Creep-feed grinding was adopted in experiments. The parameters were selected to achieve a balance between material removal rate, surface quality, and tool wear. The creep-feed grinding involves a larger cutting depth and a smaller feed speed. In order to remove the material more efficiently, while minimizing the thermal damage of the workpiece and excessive wear of the grinding wheel, the minimum cutting depth was set as 80 μm, and the change rate was 40 μm. The higher the grinding wheel speed or feed speed is, the vibration of the machine tool is increased, which makes it easy to produce workpiece burns and severe wheel wear, and the surface quality of the workpiece is poor if the grinding wheel speed is too small. Therefore, the table speeds v_w were set as 200, 300, 400, and 500 mm/min, respectively. The

grinding speed v_s was given as a constant of 31.4 m/s, and the cutting depth was set as $a_p = 80, 120, 160, \text{ and } 200 \mu\text{m}$. The workpiece is AISI 52100, and its size is 10 mm in length along the grinding direction, 10 mm in width, and 15 mm in height. The morphology evolution of the grinding wheel was observed by a 3D ultra-large depth of field microscope (VHX-5000, Keyence Ltd., Japan), and the details are shown in Fig. 1c.

3 Results and discussion

An abrasive block of the grinding wheel includes grains on the cut-in edge, cut-out edge, cylindrical surface, and side surface, as shown in Fig. 2. The cut-in edge refers to the edge of the abrasive block where it contacts initially the workpiece, and the cut-out edge is the final edge before the abrasive block moves away the workpiece surface. In

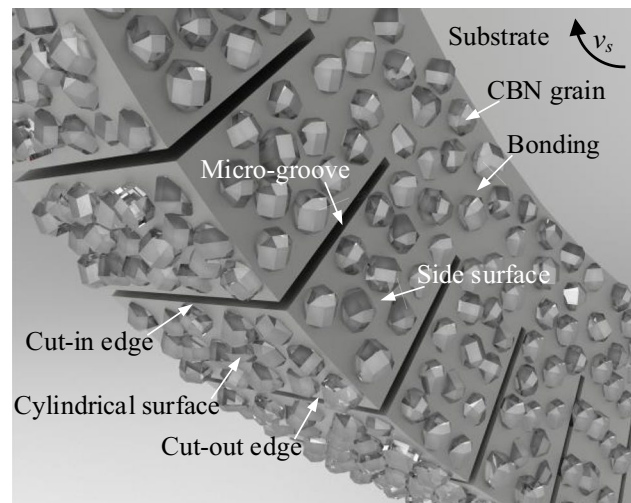


Fig. 2 Illustration of electroplated CBN grinding wheel with orderly-micro-grooves

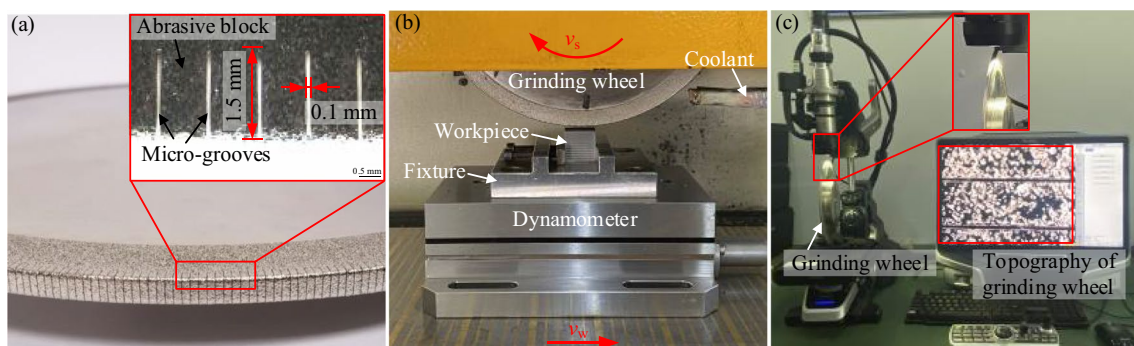


Fig. 1 Experimental setup: **a** the electroplated CBN grinding wheel with orderly-micro-grooves, **b** grinding setup, **c** characterization method of wheel topography

grinding a narrow-deep slot, the grains in different regions are engaged in the grinding process differently, and this leads to different wear behavior.

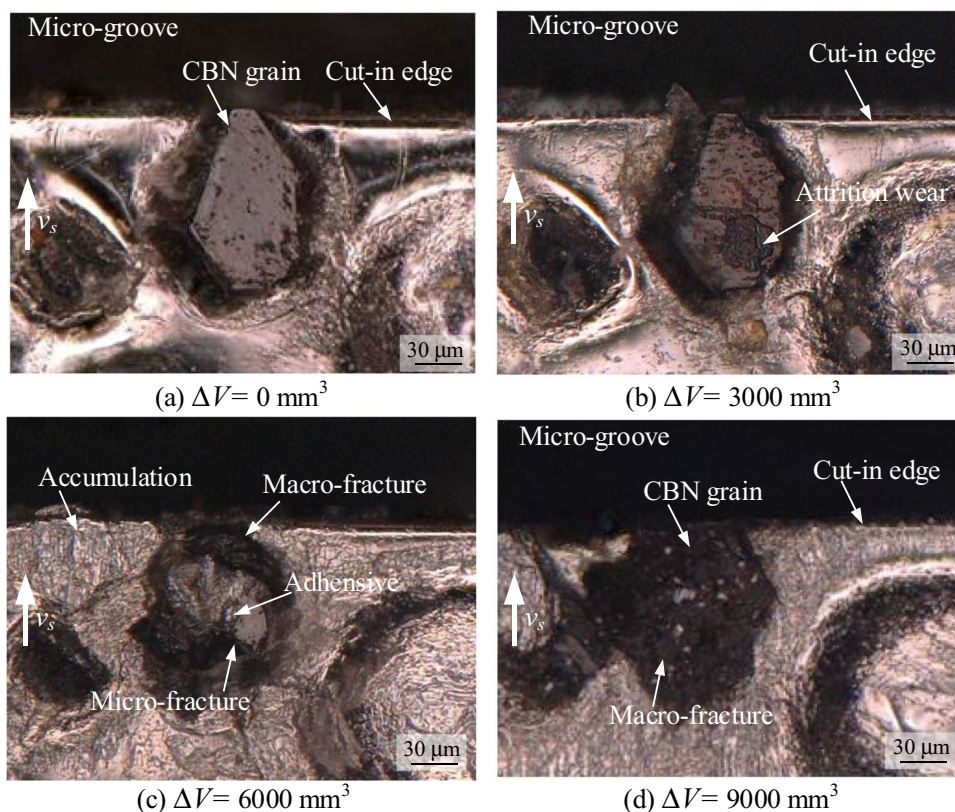
3.1 Wear behavior of grains on cut-in edge

As shown in Fig. 3, the wear morphology evolution of a typical grain on the cut-in edge is tracked with the increase in material removal volume (ΔV) ranging from 0 to 9000 mm³. As the grinding processing continues, the wear behaviors of CBN grain successively undergo attrition wear, micro-fracture, macro-fracture, chip adhesion, and accumulation. Before the grinding process, grains are firmly embedded in the nickel layer, and the average protrusion height of the grain is one-third of the grain size, as shown in Fig. 3a. Due to the high bonding strength between grains and the nickel layer, grains show excellent wear resistance. When the material removal volume reaches 3000 mm³, attrition wear occurs on the top of the grain as a small and flatted zone, and it sustains good sharpness to remove materials effectively (Fig. 3b). As the grinding process continues, the wear behaviors over grains evolved from attrition wear to micro-fracture, as shown in Fig. 3c. This is attributed to the accumulated wear of grains. As material removal volume increases, the cracks appear and expand on the CBN grain, and then, micro-fracture occurs. One cutting edge is transformed into multiple ones, and sharp cutting edges

are gradually flattened in continuing the grinding process. Even though the number of cutting edges is increased, the overall material removal rate is decreased considerably. It is observed that a small amount of chip is stuck on the top of the grain, debris accumulates in the grains, and the macro-fracture eventually occurs on the side of the micro-groove. When the material removal volume reaches 9000 mm³, the wear by macro-fracture becomes dominant, and the material loss on grain is significant, as shown in Fig. 3d. The number of effective cutting edges is decreased, and then, the shear force on the top of the active cutting edges is increased remarkably. This leads to the rapid wear of grains, and material removal ability is affected due to the lack of edge sharpness of CBN grains.

Figure 4 depicts the grinding characteristics of a grain on the cut-in edge. In comparison with the inter-grain space on the cylindrical surface, the distance from a grain on the cut-out edge of the former abrasive block to a grain on the cut-in edge of the next abrasive block is larger, and this is due to the fact that there are micro-grooves between the abrasive blocks. Therefore, the maximum undeformed chip thickness of grain on the cut-in edge is larger than that on the cylindrical surface, as shown in Fig. 4a. In comparison with a traditional grinding wheel, the micro-grooves of the wheel replace the abrasives. This causes the grinding task of the micro-grooves to be transferred to the grains on the cut-in edge of the next abrasive block. Meantime, the cutting

Fig. 3 a–d Evolution of wear morphology of a typical grain on cut-in edge



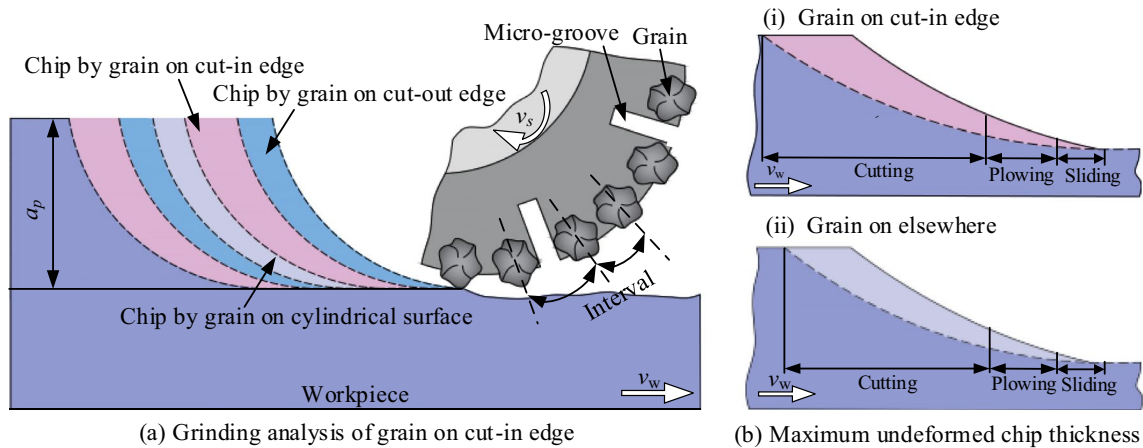


Fig. 4 a, b Grinding characteristics of grain on cut-in edge

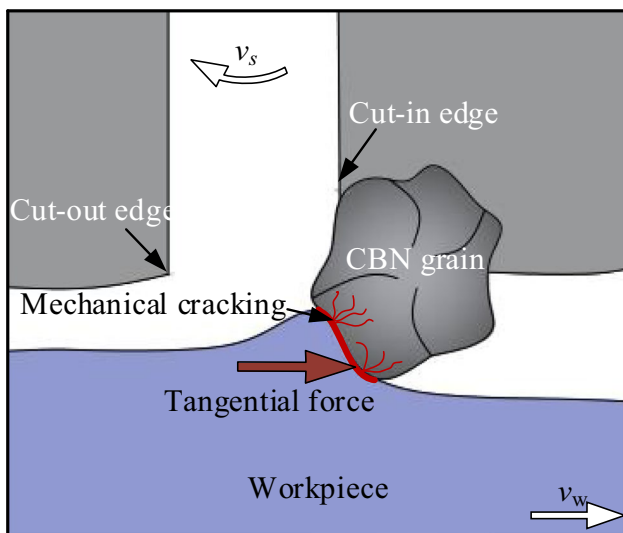


Fig. 5 Fracture mechanism of a grain on cut-in edge

length of the grain on the workpiece is proportional to its maximum undeformed chip thickness, and the cutting time of the grain on the cut-in edge is longer. Larger chip thickness and longer cutting time lead to a larger load sustained by the grain, and the grain on the cut-in edge is more likely to be fractured (Fig. 4b).

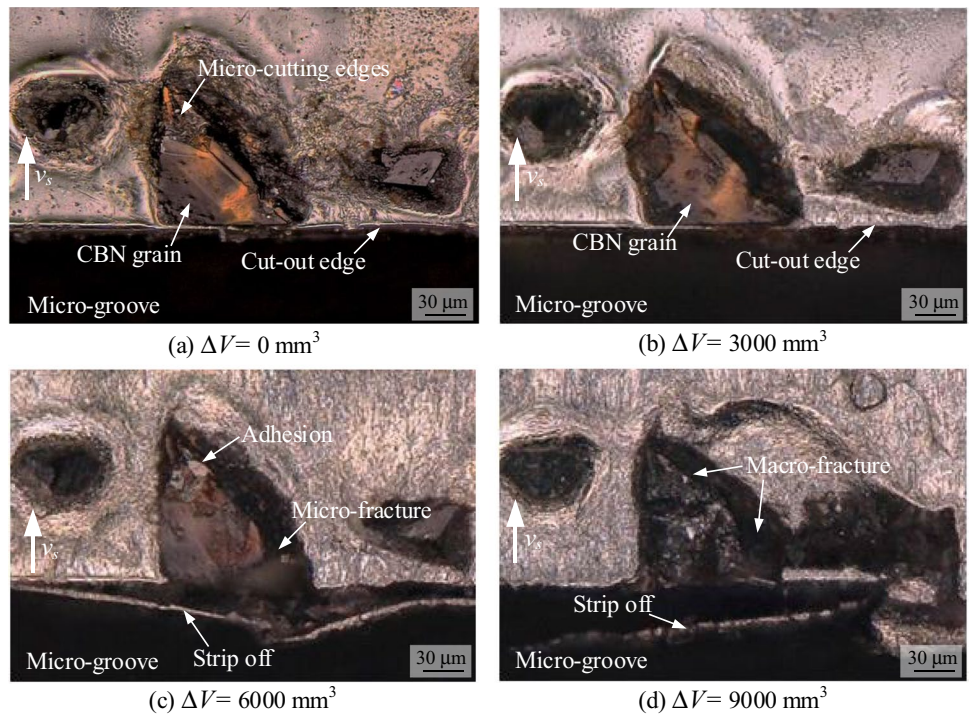
Figure 5 illustrates the fracture mechanism of the grain on the cut-in edge. For a single CBN grain, the grinding process is intermittent cutting, and then, the cutting force is periodic. The periodic cutting force acts on a grain on the cut-in edge and causes the initiation and propagation of cracks on the grain, which leads to mechanical fatigue and eventually fracture of the grain, as shown in Fig. 3c. In addition to the periodic grinding force, the thermal stress is another key factor to accelerate the fracture of grain. In an intermittent cutting, the temperature of the grain is rapidly

increased when a chip is formed. Once the grain leaves the cutting zone, it is cooled during free rotation. The thermal effect by material removal and the cooling effect by the coolant cause thermal stress of grain. The larger the difference between thermal and cooling effects is, the higher the thermal stress of the material is, and more cracks are expanded to fracture grains. In summary, with the accumulated wear of the CBN grain, the wear mechanism of grain on the cut-in edge is fractured under the combined influence of periodic cutting force and thermal stress.

3.2 Wear behavior of grains on cut-out edge

Figure 6 demonstrates the evolution of the wear morphology of a typical grain on the cut-out edge with respect to the increase of material removal volume. Figure 6a shows some sharp micro-cutting edges on the top of the original grain, and this implies an excellent material removal ability of the original grain. When the material removal volume is increased to 3000 mm³, the micro-cutting edges are worn, and attrition wear occurs on the grain. Furthermore, micro-fractures are generated on the side of the grain, and a small portion of the material is worn and torn from the grain, as shown in Fig. 6b. As the grinding process continues, the micro-cutting edges are flattened, and a small number of chips adhere to the top of the grain, as shown in Fig. 6c. This is because the flattened zone is tended to form micro-cracks subject to the grinding force, and the chips adhere to the micro-cracks easily. Meanwhile, the micro-fracture occurs near the micro-groove side, and the nickel layer on the cut-out edge is stripped off the wheel hub. When the material removal volume is increased to 9000 mm³, the loss of grain material is significant, and macro-fracture occurs, as shown in Fig. 6d. This is attributed to the chip adhesion that increases the local cutting loads on the top of the grain; micro-cracks are propagated to accelerate the wear of

Fig. 6 a–d Wear behavior of a typical grain on cut-out edge

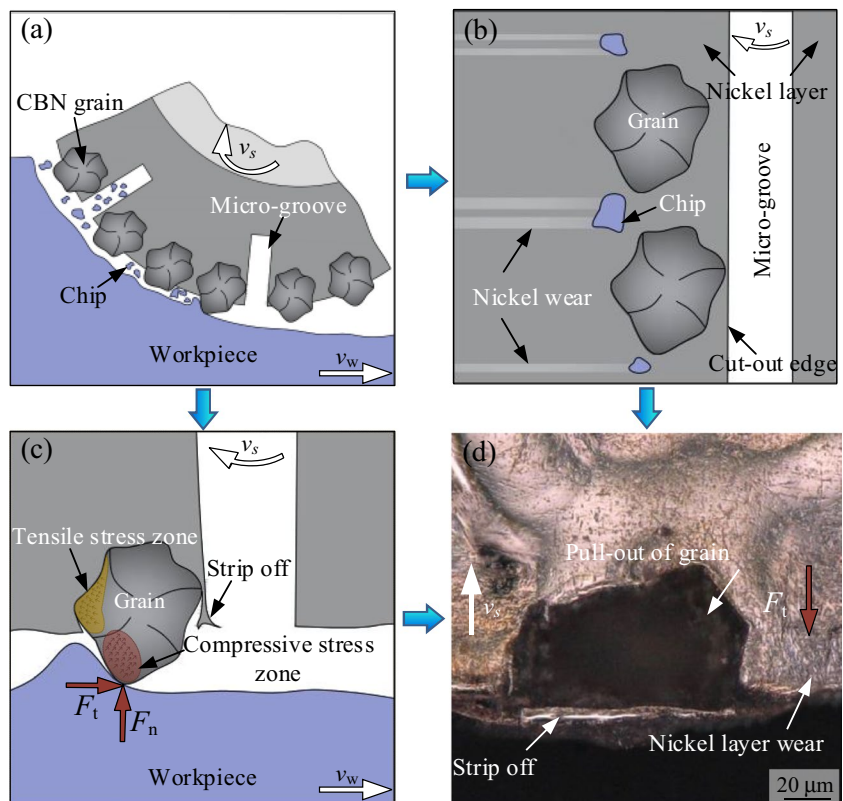


grain and, eventually, the fractures of the grain. In addition, the stripping of the nickel layer on the cut-out edge is very severe and weakens the mechanical anchorage between the CBN grain and the nickel layer. The grain on the cut-out

edge is easily pulled out. In such a case, the material removal ability is reduced considerably.

Figure 7 shows the wear mechanism of grain on the cut-out edge. Hard-brittle chips are generated in the grinding

Fig. 7 a–d Wear mechanism of grain on cut-out edge



zone, and most of these chips are either washed away by coolant or stored in the micro-grooves, as shown in Fig. 7a, while a small portion of chips freely rolls or slides in the grinding zone. These free chips act as micro-tools subject to mutual squeeze between the grinding wheel and the workpiece to slide, plow, and cut the nickel layer (Fig. 7b), which reduces the embedment depth of the grains. Furthermore, the interaction between the workpiece and the grain produces a compressive pressure over the grain and leads to residual stress inside the grain. Under the squeezing and friction of the workpiece material, the concentration of the compressive pressure appears on the rake face of the grain, and this leads to crack initiation and grain fractures. With the applied tangential grinding force (F_t), tensile stress occurs at the interface of the grain and nickel layer, as illustrated in Fig. 7c. Since the micro-groove cannot provide support for the cut-out edge, the nickel layer is stripped off the wheel hub easily subjected to a tangential grinding force. The stripping of the nickel layer reduces the anchoring force of the grain on the cut-out edge and further aggravates the tendency of grain pull-out. With an increase of the wear induced by tangential cutting force, the grain is overturned and pulled out from the grinding wheel, as shown in Fig. 7d.

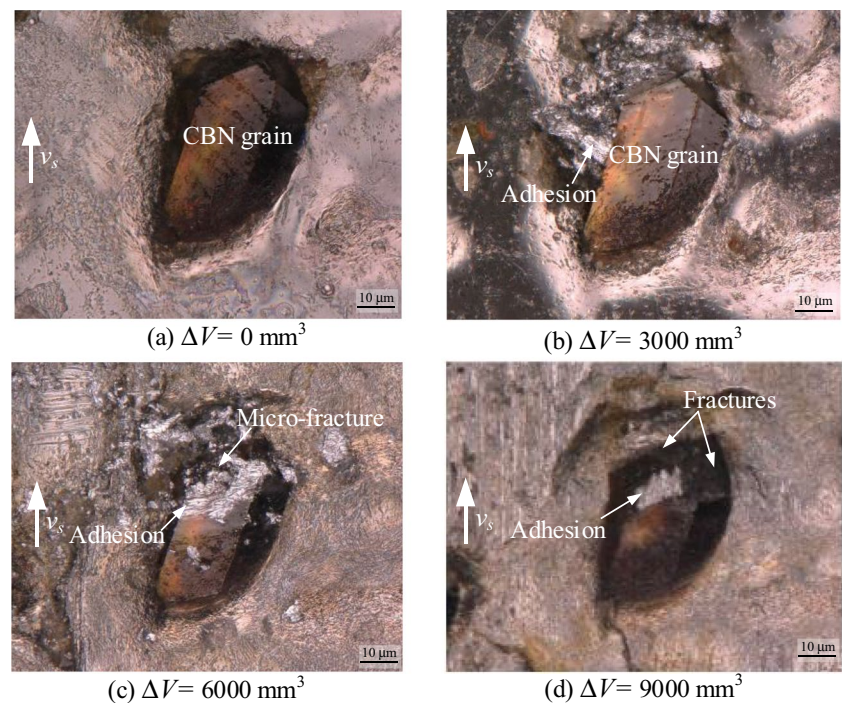
In summary, the wear of the nickel layer increases the protrusion height of grains, and the stripping of the nickel layer from the cut-out edge reduces the anchorage force of grains, thus causing the pull-out of the grains on the cut-out edge.

3.3 Wear behavior of grains on cylindrical surface

The wear evolution of grain on the cylindrical surface at different material removal volumes is shown in Fig. 8. Figure 8a shows that the cutting edges of an original grain are sharp so the material removal ability is excellent. As the material removal volume increases to 3000 mm^3 , the chip adhesion is generated on the side of the grain (Fig. 8b). When the material removal volume reaches 6000 mm^3 , an amount of chip is stuck on the top of the grain, and micro-fractures occur on the rake face of the grain, as shown in Fig. 8c. It is ascribed that the generated chips in the grinding zone are softened at high temperature, and then, these chips easily adhered to the rake face of grain. The chip adhesion reduces the sharpness of the grain and increases the cutting force on the grain, which leads to the micro-fracture over the rake face of the grain. Thus, the corresponding material removal ability is decreased. When the material removal volume increases to 9000 mm^3 , some fractures on the grain appear, and the area of chip adhesion on the grain is reduced (Fig. 8d).

Figure 9 explains the formation mechanism of adhesion. Grinding involves the interaction of micro-asperities of grain and workpiece, and the actual contact area among micro-asperities is small. The contact interfaces are severely compressed with high stress and high temperature under the action of grinding force, and micro-welds are formed easily, as shown in Fig. 9b. The large number of micro-welds causes material bonding at the contact interface, which resists the

Fig. 8 a–d Grain wear evolution on cylindrical surface



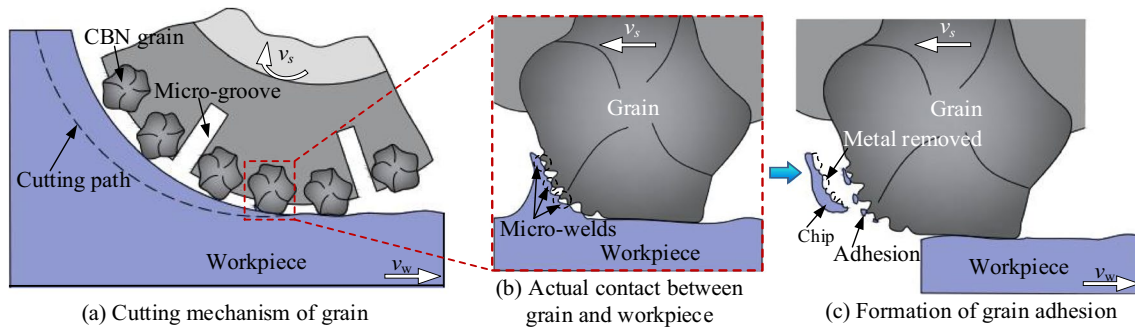


Fig. 9 a–c Formation mechanism of grain adhesion

sliding motions of the grains and the workpiece. As a result, Workpiece materials are removed under the squeezing effect of grains, and some of them are attached to the grains by the adhesion of micro-welds, as shown in Fig. 9c.

In the grinding process, the chips stuck in an inter-grain space are not washed away by coolant. These chips are softened by high grinding temperature and gradually adhere to the rake face of grain by micro-welds. Then, the loaded grain enforces the chips to flow across the rake face and increases the adhesion of the chips. In creep-feed grinding, the large cutting depth increases the contact area between the wheel and workpiece in comparison with that in traditional grinding, and this increases the effective length for grains to slide

over the workpiece. Then, the chip adhesion on the rake face of the grain is more serious. An electroplated wheel usually exhibits a random distribution of grains, and the geometries and intervals of grains are stochastic. The 3D ultra-large depth of field microscope is used to observe the surface of the grinding wheel, and Fig. 10 shows that chip adhesions are divided into two cases according to the inter-grain space.

When the inter-grain space is small (Fig. 10a), the chip adhesion is initiated on the rake face of the grains. Since the spacing of two grains is small, the adhesion enters an inter-grain space and then bridges two adjacent grains. Through chip-to-chip adhesion and deposition, the adhesion is extended to adjacent grains. A large range of bridge

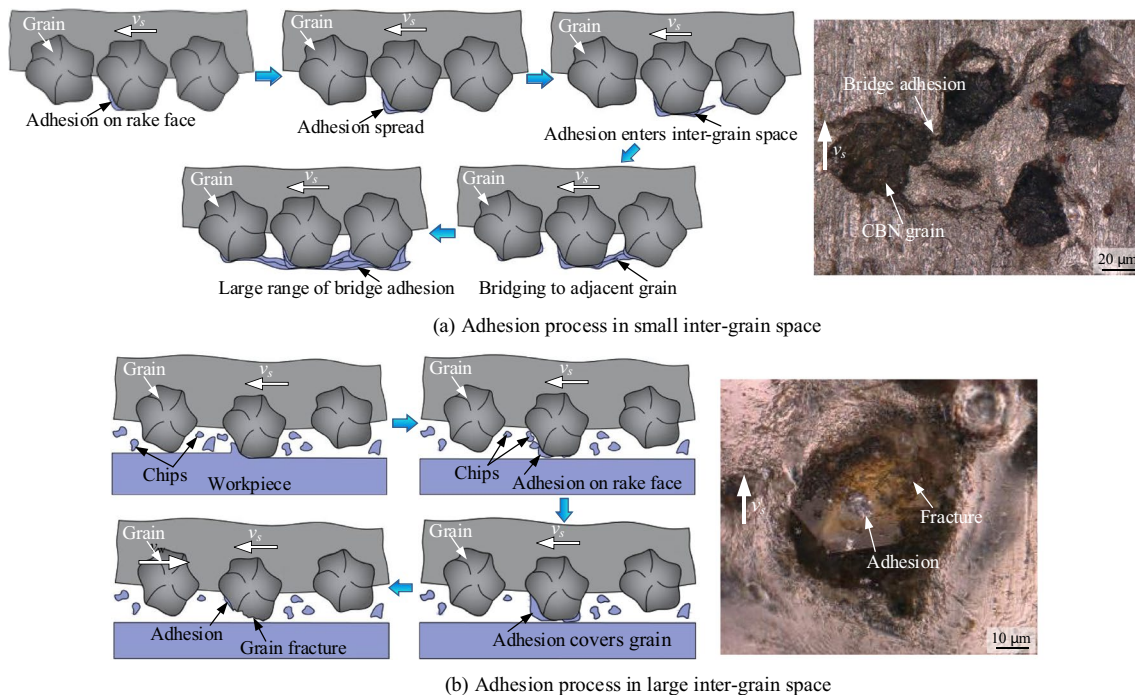


Fig. 10 a, b Adhesion process of chips in different inter-grain spaces

adhesions is formed, and the cutting edges of grains are covered to cause resistance to material removal. It results in the deteriorated grinding performance of grains.

Figure 10b shows the case with a large inter-grain space. The chip adhesion gradually covers the grain, and the grain becomes blunt and thus aggravates sliding and plowing. The tangential force is increased due to attrition wear on grains and concentrated stresses, and this accelerates crack initiation and propagation. The grains are fractured before the adhesion is developed to bridge grains, so the adhesion occurs on a single grain. The fractured grain generates new sharp cutting edges, which reduces the chip adhesion and improves the material removal ability, and finally realizes the self-sharpening characteristics of grain. In summary, the creep-feed grinding aggravates the sliding effect of grains, and the wear of grains on the cylindrical surface is primarily caused by chip adhesion.

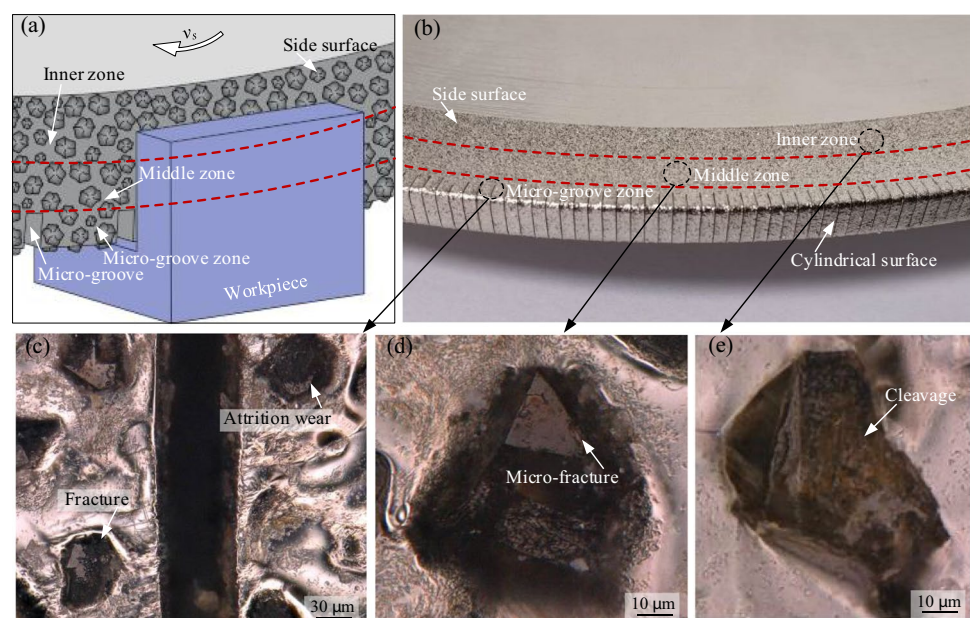
3.4 Wear behavior of grains on side surface

Figure 11 shows the wear characteristics of grains on the side surface. In the grinding of the narrow-deep slot, the grains on the cylindrical surface are not able to remove all workpiece materials due to the large cutting depth. Part of the material is put aside on two sides of the wheel and eventually removed by the grains on the side surface. The cutting depth of grains on the side surface is gradually reduced along the radial direction of the wheel. Depending on the radial distance of a zone to the center of the wheel, the side surface of the wheel can be divided into a micro-groove zone, middle zone, and inner zone. The micro-groove zone is characterized by the micro-grooves located on the outside of the grinding wheel. The inner zone is located closer

to the center of the grinding wheel and is least affected by workpiece wear. The middle zone is located between the micro-groove zone and the inner zone. The grains in the micro-groove zone undertake the main material removal task of the side surface, while the cutting depths of the grains in the middle and inner zones are close to zero. Under this thin cutting depth, grains are not squeezed into the workpiece material; instead, these grains merely slide and plow on the workpiece surface, and the amount of removed materials is extremely limited. Therefore, grains on different grinding zones show different wear modes.

Figure 11(b–e) shows the worn morphology of grains on the side surface. The wear behavior of the grains in the micro-groove zone is dominated by attrition wear and micro-fracture. This can be explained that the cutting depth of the grains in the micro-groove zone is larger than those in the inner or middle zones. The grains are sliding, and the attrition wear occurs to form a wear-flatten area on the top of the grains. When the worn area is increased to a certain extent, the grain is fractured. Moreover, a small number of scratches occurred on the nickel layer. The wear behavior of grains in the middle zone is micro-fracture on the top of grains. With the continuation of the grinding process, the ground depth of the narrow-deep slot is increased, and more grains in the middle zone are engaged in grinding. The number of active grains is increased, and this increases the tangential grinding force and accordingly causes the micro-fracture on the top of the grains in the middle zone. The wear of the grains in the inner zone is manifested as cleavage. Due to the high-speed rotation of the wheel and the scouring of coolant, micro-vibrations of the grinding wheel are inevitable. The micro-vibrations make some grains in the inner zone contact the sides of the narrow-deep slot. The friction at contact

Fig. 11 Wear characteristics of grain on side surface



increases and fluctuates the grinding force. When the tensile stress in the grain exceeds its tensile strength, a cleavage fracture occurs on the grain in the inner zone.

3.5 Comparative analysis of grinding forces

Figure 12 displays the grinding ratio of the orderly-micro-grooved grinding wheel and the traditional grinding wheel versus the accumulative material removal in grinding narrow-deep slot. With the workpiece material removal volume increasing, the grinding ratio G shows a trend of increasing, then decreasing, and then becoming stable. When the accumulative material removal volume is 6500 mm^3 , the grinding ratio of the traditional grinding wheel reaches the

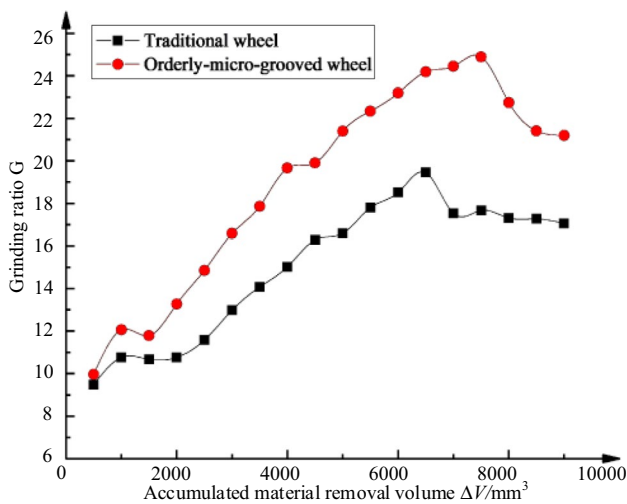
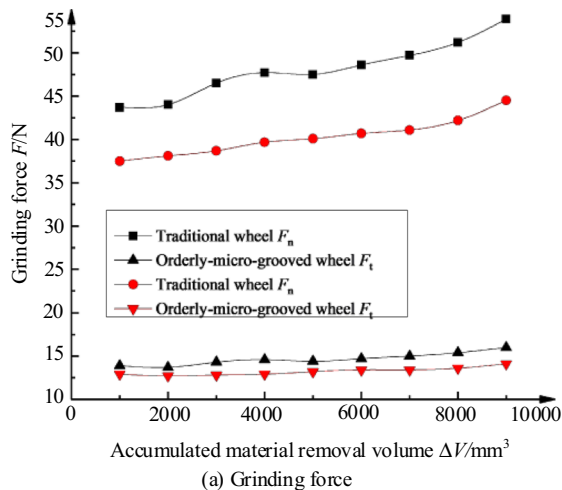
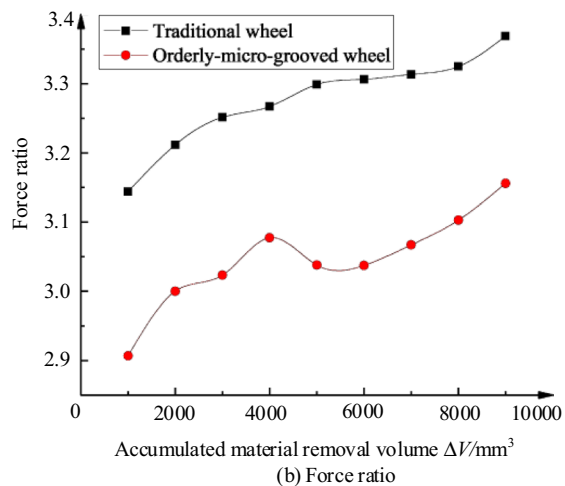


Fig. 12 Grinding ratio of grinding wheel against the accumulative material removal volume



(a) Grinding force



(b) Force ratio

Fig. 13 a, b Variation of grinding force and force ratio with the accumulative material removal volume

highest and then decreases rapidly. Combined with the wear behavior of the traditional wheel of grinding narrow-deep slot [33], the large range of chip adhesion and wheel loading are important factors leading to the rapid reduction of the grinding ratio of the traditional wheel. In contrast, the orderly-micro-grooved grinding wheel from the early wear stage shows a high grinding ratio, and the grinding ratio begins to decrease when the cumulative material removal volume reaches 7500 mm^3 . The grinding ratio of the grinding wheel with orderly-micro-grooves is about 1.3 times that of the traditional grinding wheel. This is because the grain on the cut-in edge wear behavior is more likely to show sharp cutting edges, making the orderly-micro-grooved wheel maintain a good sharpness during a long grinding process. The self-sharpening characteristics of the grains on the cylindrical surface show the excellent wear resistance of the orderly-micro-grooved grinding wheel in the grinding process.

The variation of grinding force and force ratio with the accumulative removal volume is depicted in Fig. 13. As the accumulative material removal volume increases from 0 to 9000 mm^3 , the normal and tangential grinding forces of the two grinding wheels increase to varying degrees (Fig. 13a). It is worth noting that the tangential and normal grinding forces of the orderly-micro-grooved wheel are less than that of the traditional grinding wheel. The main reason for this phenomenon is the large number of micro-grooves distributed on the working surface of the grinding wheel, which makes intermittent contact between the grinding wheel surface and the workpiece. Compared with the traditional grinding wheel, the orderly-micro-grooved wheel has fewer active grains in contact with workpieces, and the contact length is smaller, leading to the grinding force being smaller.

Figure 13b reflects the trend of the grinding force ratio of the two grinding wheels with the accumulative material removal volume. As the accumulative material removal volume ranged from 0 to 4000 mm³, the grinding force ratio of the orderly-micro-grooved wheel increased from 2.90 to 3.07, indicating that attrition wear occurred at this stage, and the sharp cutting edge was worn. With the accumulative material removal volume reaching 6000 mm³, the grinding force ratio decreases to 3.03. This manifests that micro-fracture occurs at this stage, and newly sharp cutting edges appear and show good self-sharpness of the grinding wheel. Subsequently, the grinding force ratio increases, indicating that the number of sharp cutting edges is decreased, and the sharpness of the orderly-micro-grooved wheel is reduced. In contrast, the increasing grinding force ratio of the traditional grinding wheel reflects the continuous decrease in the sharpness of the grinding wheel. It reflects that the self-sharpening ability of the traditional grinding wheel is limited, and the sharpness of the grinding wheel cannot be maintained for a long time during the grinding process. The comparative analysis of grinding force and force ratio further verifies the excellent grinding performance of the orderly-micro-grooved wheel in grinding narrow-deep slot.

4 Conclusion

The wear behavior of the grinding wheel with orderly-micro-grooves in grinding narrow-deep slots is investigated. The wear morphology of grains on the cut-in edge, cut-out edge, cylindrical surface, and side surface is observed. The variations of grinding ratio, grinding force, and force ratio with the accumulative material removal volume are analyzed.

The results show that the micro-grooves influence the wear behaviors of the grinding wheel. The micro-grooves of the grinding wheel replace abrasive, and a portion of material removal is shifted to the grains on the cut-in edge of the next block. This increases the maximum undeformed chip thickness of the grains on the cut-in edge. The increased chip thickness increases the cutting load over the grains and causes macro-fractures of the grains on the cut-in edge. The micro-groove cannot provide support for the cut-out edge, and the nickel layer is easily stripped off the wheel hub under the action of the tangential grinding force. This reduces the anchorage force of grains with the nickel layer and aggravates the tendency of the grains on the cut-out edge to be pulled out. In creep-feed grinding, micro-welds are formed easily at the contact interfaces between the grains and the workpiece under the action of high grinding stress and temperature. A portion of workpiece materials is stuck on the grains by micro-welds. The wear of grains on the cylindrical surface is mainly by adhesion, and the adhesion is prone to

bridge at the small inter-grain spaces. Therefore, increasing the spacing between grains in the preparation process of the grinding wheel can effectively reduce the adhesion area. The grains on the side surface remove less workpiece material, and the cutting depths of the grains in the middle or inner zones are close to zero; therefore, the wear of the grains on the side surface is insignificant. The wear behavior of the grain on the side surface is attrition wear or micro-fractures.

The grinding ratio of the grinding wheel with orderly-micro-grooves is 1.3 times that of the traditional wheel, and this reveals that the orderly-micro-grooved grinding wheel has stronger wear resistance. The grinding force and force ratio variation further verifies that the orderly-micro-grooved grinding wheel can achieve self-sharpening to maintain excellent grinding performance. This confirms the feasibility and superiority of the grinding wheel with orderly-micro-grooves during grinding narrow-deep slots.

Author contributions All authors contributed to the study conception and design. Material preparation, data collection, and analysis were performed by C.M. and X.L. The first draft of the manuscript was written by C.M. and X.L., and all authors commented on previous versions of the manuscript. All authors read and approved the final manuscript.

Funding The present research work was sponsored by the National Natural Science Foundation of China (Grant Nos. 52275405, 52275311, 51875050), the Hunan Province Science and Technology Innovation Program (Grant No. 2023RC1078), and the Changsha City Science and Technology Innovation Program (Grant No. kh2301003).

Declarations

Conflict of interest The authors declare no competing interests.

References

- Bai YY, Lv M, Li WB, Liang GX (2017) An experimental study on the creep feed grinding of narrow deep grooves of stainless steel. *Int J Adv Manuf Technol* 90:1835–1844
- Wang JW, Yu TY, Ding WF, Fu YC, Bastawros AF (2018) Wear evolution and stress distribution of single CBN superabrasive grain in high-speed grinding. *Precis Eng* 54:70–80
- Li HN, Axinte D (2016) Textured grinding wheels: a review. *Int J Mach Tool Manuf* 109:8–35
- Guo B, Zhao QL, Fang XY (2014) Precision grinding of optical glass with laser micro-structured coarse-grained diamond wheels. *J Mater Process Technol* 214(5):1045–1051
- Denkena B, Grove T, Göttching T, Silva EJ, Coelho RT, Filleti R (2015) Enhanced grinding performance by means of patterned grinding wheels. *Int J Adv Manuf Technol* 77:1935–1941
- Shi CF, Li X, Chen ZT (2014) Design and experimental study of a micro-groove grinding wheel with spray cooling effect. *Chin J Aeronaut* 27(2):407–412
- Tawakoli T, Heisel U, Daneshi A (2012) An experimental investigation on the characteristics of cylindrical plunge dry grinding with structured cBN wheels. *Procedia CIRP* 1:399–403

8. Aurich JC, Kirsch B, Herzenstiel P, Kugel P (2011) Hydraulic design of a grinding wheel with an internal cooling lubricant supply. *Prod Eng* 5:119–126
9. Walter C, Komischke T, Kuster F (2014) Laser-structured grinding tools-generation of prototype patterns and performance evaluation. *J Mater Process Technol* 214(5):951–961
10. Mohamed A-MO, Bauer R, Warkentin A (2013) Application of shallow circumferential grooved wheels to creep-feed grinding. *J Mater Process Technol* 213(5):700–706
11. Oliveira JFG, Bottene AC, França TV (2010) A novel dressing technique for texturing of ground surfaces. *CIRP Ann Manuf Technol* 59(1):361–364
12. Ding WF, Zhao B, Zhang QL, Fu YC (2021) Fabrication and wear characteristics of open-porous CBN abrasive wheels in grinding of Ti-6Al-4V alloys. *Wear* 477:203786
13. Xiao GD, Zhao B, Ding WF, Huan HX (2021) On the grinding performance of metal-bonded aggregated CBN grinding wheels based on open-pore structures. *Ceram Int* 47(14):19709–19715
14. Cao Y, Ding WF, Zhao B, Wen XB, Li SP, Wang JZ (2022) Effect of intermittent cutting behavior on the ultrasonic vibration-assisted grinding performance of Inconel718 nickel-based superalloy. *Precis Eng* 78:248–260
15. Yuan HP, Gao H, Bao YJ, Wu Y (2009) Grinding of carbon/epoxy composites using electroplated CBN wheel with controlled abrasive clusters. *Key Eng Mater* 389:24–29
16. Mao C, Long P, Tang WD, Xiao LF, Luo YQ, Shu ZR, Hu YL, Bi ZM, Lin ZH, Guan FR (2022) Simulation and experiment of electroplated grinding wheel with orderly-micro-grooves. *J Manuf Process* 79:284–295
17. Upadhyaya RP, Fiecoat JH (2007) Factors affecting grinding performance with electroplated CBN wheels. *CIRP Ann* 56(1):339–342
18. Gift FC, Misiolok WZ (2004) Fluid performance study for groove grinding a nickel based superalloy using electroplated cubic boron nitride grinding wheels. *J Manuf Sci Eng* 126(3):451–458
19. Cao Y, Yin JF, Ding WF, Xu JH (2021) Alumina abrasive wheel wear in ultrasonic vibration-assisted creep-feed grinding of Inconel 718 nickel-based superalloy. *J Mater Process Technol* 297:117241
20. Cao Y, Zhu YJ, Li HN, Wang CX, Su HH, Yin Z, Ding WF (2020) Development and performance of a novel ultrasonic vibration plate sonotrode for grinding. *J Manuf Process* 57:174–186
21. Hartig J, Kirsch B, Aurich JC (2022) Analysis of the grinding wheel wear and machining result during cutting edge preparation with elastic bonded grinding wheels. *J Manuf Process* 75:181–202
22. Zhang ZC, Sui MH, Li CH, Zhou ZM, Liu B, Chen Y, Said Z, Debnath S, Sharma S (2022) Residual stress of grinding cemented carbide using MoS₂ nano-lubricant. *Int J Adv Manuf Technol* 119:5671–5685
23. Azizi A, Rezaei SM, Rahimi A (2010) Study on the rotary cup dressing of CBN grinding wheel and the grinding performance. *Int J Adv Manuf Technol* 47:1053–1063
24. Naik DN, Mathew NT, Vijayaraghavan L (2019) Wear of electroplated super abrasive CBN wheel during grinding of Inconel 718 super alloy. *J Manuf Process* 43:1–8
25. Shi Z, Malkin S (2006) Wear of electroplated CBN grinding wheels. *J Manuf Sci Eng* 128(1):110–118
26. Miao Q, Ding WF, Kuang WJ, Xu JH (2020) Tool wear behavior of vitrified microcrystalline alumina wheels in creep feed profile grinding of turbine blade root of single crystal nickel-based superalloy. *Tribol Int* 145:106144
27. Miao Q, Ding WF, Xu JH, Cao LJ, Wang HC, Yin Z, Dai CW, Kuang WJ (2021) Creep feed grinding induced gradient microstructures in the superficial layer of turbine blade root of single crystal nickel-based superalloy. *Int J Extreme Manuf* 3:045102
28. Naskar A, Choudhary A, Paul S (2020) Wear mechanism in high-speed superabrasive grinding of titanium alloy and its effect on surface integrity. *Wear* 462:203475
29. Li BK, Yin JF, Zhu YJ, Zhang X, Ding WF (2021) Grain wear evolution of cubic boron nitride abrasives during single grain grinding of powder metallurgy superalloy FGH96. *Ceram Int* 47(2):2508–2516
30. Liu MZ, Li CH, Zhang YB, Yang M, Gao T, Cui X, Wang XM, Xu WH, Zhou ZM, Liu B, Said Z, Li RZ, Sharma S (2023) Analysis of grinding mechanics and improved grinding force model based on randomized grain geometric characteristics. *Chin J Aeronaut* 36(7):160–193
31. Li P, Jin T, Xiao H, Chen ZQ, Qu MN, Dai HF, Chen SY (2020) Topographical characterization and wear behavior of diamond wheel at different processing stages in grinding of N-BK7 optical glass. *Tribol Int* 151:106453
32. Zhu YJ, Ding WF, Rao ZW, Fu YC (2019) Effect of grinding wheel speed on self-sharpening ability of PCBN grain during grinding of nickel-based superalloys with a constant undeformed chip thickness. *Wear* 426:1573–1583
33. Li G, Liang GX, Shen XQ, Lv M, Liu DG, Hao XH, Huang YG, Tochukwu OP, Al-Nehari M (2021) Investigation of the wear behavior of abrasive grits in a dry machining Inconel 718 narrow-deep-groove with a single-layer cubic boron nitride grinding wheel. *Int J Adv Manuf Technol* 117:1061–1076

Publisher's Note Springer Nature remains neutral with regard to jurisdictional claims in published maps and institutional affiliations.

Springer Nature or its licensor (e.g. a society or other partner) holds exclusive rights to this article under a publishing agreement with the author(s) or other rightsholder(s); author self-archiving of the accepted manuscript version of this article is solely governed by the terms of such publishing agreement and applicable law.